Structure and strong ultraviolet emission characteristics of amorphous ZnO films grown by electrophoretic deposition

Zhijian Wang, Haiming Zhang, Zhijun Wang, Ligong Zhang, and Jinshan Yuan
Laboratory of Excited State Processes, Chinese Academy of Sciences, Changchun Institute of Optics, Fine Mechanics and Physics, Chinese Academy of Sciences, Changchun 130021, People's Republic of China

Shenggang Yan and Chunyan Wang
School of Chemical Engineering, Dalian University of Technology Dalian, 116012 People's Republic of China

(Received 1 July 2002; accepted 17 October 2002)

Structure and ultraviolet emission characteristics of amorphous ZnO films grown on indium tin oxide coated glass substrates by electrophoretic deposition were investigated using Raman spectra and photoluminescence. The Raman spectrum shows a unique resonant multiphonon process within amorphous ZnO films. The photoluminescence spectrum of amorphous ZnO films shows a strong ultraviolet emission while the visible emission is nearly fully quenched. The transmission electron microscopy, x-ray diffraction, x-ray photoelectron spectrum, and infrared spectrum are used to detect the structure of amorphous ZnO powder. The complex water plays an important role in the photoluminescence intensity emission.

I. INTRODUCTION

There has been great interest in wide band gap semiconductors because there is a strong commercial desire to produce efficient and lasing blue light-emitting diodes and short-wavelength laser diodes. As a wide band gap (E_g = 3.37 ev[1]) semiconductor material, ZnO has received an increasing amount of attention due to its possible application in ultraviolet (UV) light-emitting devices,[2,3] electron-acoustic devices,[4] UV detectors,[5] and others.[6] In recent years, there has been a great interest in the development of high-quality ZnO films to obtain strong UV emission. Several techniques are being used to produce ZnO film; e.g., metalorganic chemical vapor deposition,[7] molecular beam epitaxy,[8] chemical vapor deposition,[9] combustion chemical vapor deposition,[10] pulsed laser deposition, [11] and electrophoretic deposition (EPD).[12,13] The main advantages of EPD are easy operation and no need for complex instruments.

In most previous works, visible emission dominated the photoluminescence (PL) spectra of ZnO films. Few PL spectra of ZnO films with pure strong UV have been reported.[14] In this article, we first report a simple and efficient method to prepare amorphous ZnO powder by solid-state pyrolytic reaction; then the amorphous ZnO films were deposited onto indium tin oxide (ITO) coated glass substrates by EPD. The amorphous ZnO displayed quasi-three-dimensional quantum confinement effects, greatly increasing the PL efficiency. PL spectra indicated that the EPD films of amorphous ZnO appeared to have strong UV emission, while that visible emission was barely observed at room temperature.

II. EXPERIMENTAL

A. Electrophoretic deposition of amorphous ZnO films

The preparation of amorphous ZnO films is described as the following. Deposition solution was prepared with concentration of 0.006 M amorphous ZnO and 10^{-5} M of $Mg(NO_3)_2 \cdot 6H_2O$ in isopropyl alcohol solvent. Here, preparation of amorphous ZnO powder can be briefly described as follows: 2.2 g (10 mmol) $Zn(CH_3COO)_2 \cdot 2H_2O$ and 2 g (23.8 mmol) $NaHCO_3$ were mixed at room temperature. The reaction mixture was pyrolytized at 160 °C for 3 h. The $Zn(CH_3COO)_2 \cdot 2H_2O$ changed into amorphous ZnO, while the $NaHCO_3$ changed into CH_3COONa and was eventually washed away by deionized water. Consequently, a white, highly fluffy, voluminous, floccular, amorphous ZnO (0.94 g) can be obtained through the solid-state thermal decomposition process. A stainless steel sheet and an ITO-coated glass slide with a deposition area of 2 cm^2 were used as the anode and cathode, respectively. The electrodes were placed parallel to each other separated by a distance of approximately 3 cm and immersed into the deposition solution. Film deposition experiments were performed at a constant current of

10 mA for 10 min at ambient conditions. After deposition, the films were removed from the deposition solution and then dried at 100 °C. Uniform and white amorphous ZnO films can be obtained.

B. Characterization

Transmission electron microscopy (TEM) images were taken on a JEOL-2010 TEM (Tokyo, Japan) operated at 200 Kv.

The x-ray diffraction (XRD) spectra was performed on the ZnO films using a D/max-rA XRD spectrometer (Rigaku, Tokyo, Japan) with a Cu K_α line of 1.54 Å.

X-ray photoelectron spectra (XPS) measurements were performed on a VG Scientific Escalb Mark II (France) instrument, using a monochromatized Al (K_α) source. The pressure in the chamber was 5×10^{-8} mbar. For final calibration of the energy scale, the C (1*s*) peak was set to 284.6 ev.

Infrared (IR) absorption spectra were collected on a Shimazu FT-IR 8200D (Japan) spectrometer.

To study the luminescence properties of the amorphous ZnO films, the PL spectra of amorphous ZnO were recorded with a Hitachi MPF-4 (Tokyo, Japan) fluorescence spectrophotometer. The spectra were obtained by exciting the sample with a Xe lamp as the excitation light source at the room temperature. The wavelength was 325 nm. The Raman spectra measurements were carried out using a Microlaser Raman spectrometer (Jolin Won Co., France).

III. RESULTS AND DISCUSSION

A typical TEM image of amorphous ZnO is shown in Fig. 1. The image shows that the amorphous ZnO is distributed disorderly and does not have distinct morphology. When we tried to obtain selected-area electron diffraction patterns, we could not obtain an image. Clearly, the crystal ZnO was not formed at that time. To confirm that the sample is amorphous ZnO, XRD was also used to characterize the sample. XRD probed a large number of crystallites that were statistically oriented. Experimental XRD spectra for amorphous ZnO are shown in Fig. 2. Figure 2(a) shows only some weak diffraction peaks, which are not obvious oriented.

Figures 3(a) and 3(b) show the XPS of amorphous ZnO powder. Binding energies of O(1*s*), Zn($2p_{1/2}$), and Zn($2p_{3/2}$) provided a rather complete picture of sample powder. The Zn($2p_{3/2}$) XPS appearing at 1021.8 ev coincides with ZnO data. The O(1*s*) peak at 531.5 ev is attributed to oxide ions in ZnO. The peaks corresponding to $Zn(OH)_2$ and other basic salts are absent. An IR spectrum of sample is shown in Fig. 3. The weak peak at 472 cm^{-1} is due to the ZnO stretching mode, but additional vibrations are present around 842, 1047, 1386, 1460, 1501, and 3403 cm^{-1}. The peaks at 842 and 1047 cm^{-1}, and the strong peaks at 1386, 1460, and 1501 cm^{-1} are attributed to symmetric and asymmetric bending and stretching modes of $ZnO \cdot H_2O$,

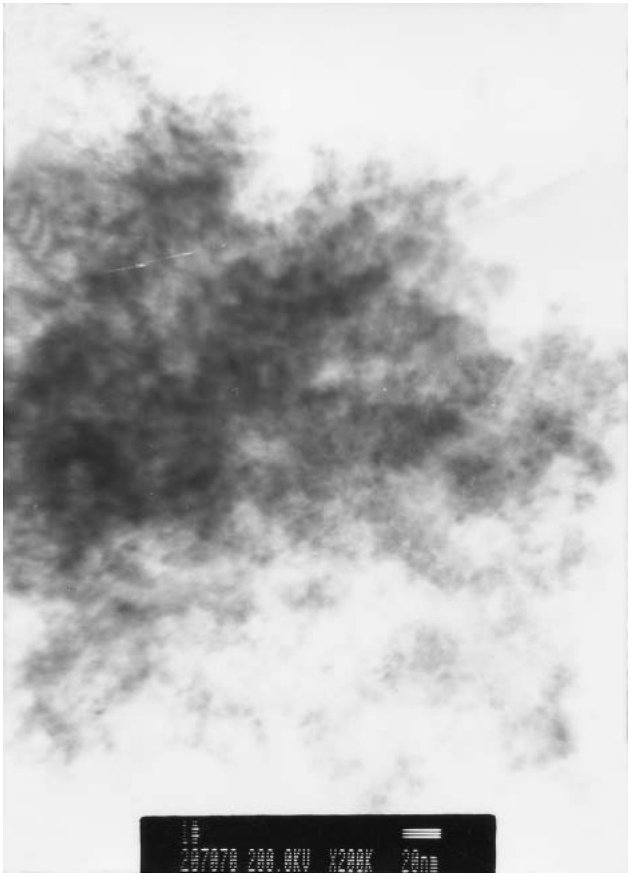

FIG. 1. TEM image of amorphous ZnO. Imaging at $200*10^3$ times magnification.

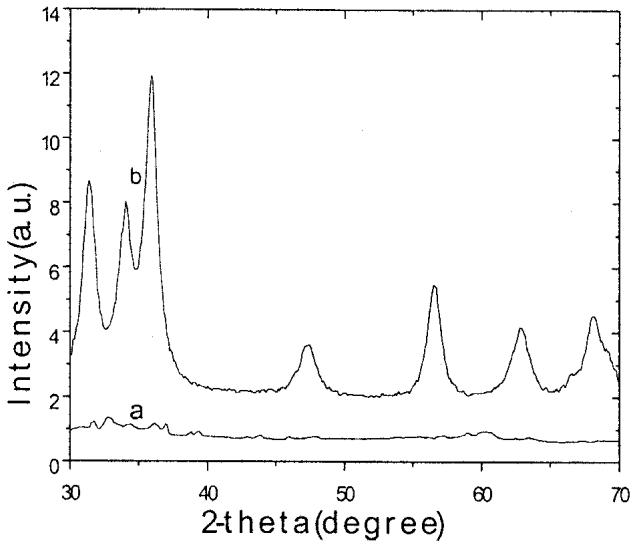

FIG. 2. X-ray powder diffraction patterns of ZnO. (a) Amorphous ZnO (b) Nanocrystalline ZnO for comparision. The scan conditions were 1/2 degree every minute.

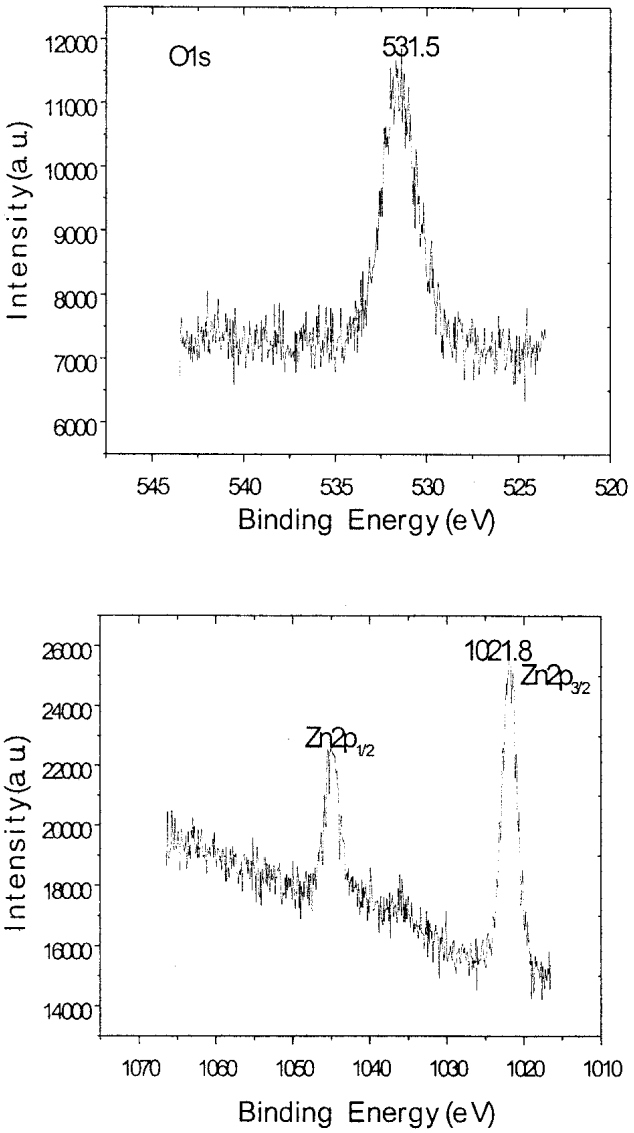

FIG. 3. O1s and Zn2p XPS of amorphous ZnO.

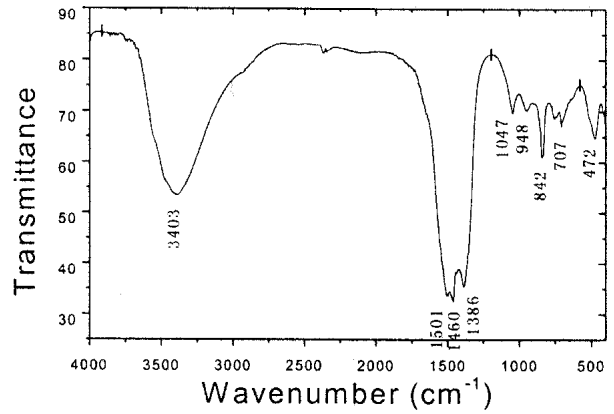

FIG. 4. IR spectrum of amorphous ZnO.

respectively. The peak at 3403 cm^{-1} can be indexed as vibration of H_2O. The absence of the frequency in the region of 1600 cm^{-1} indicates that there is no absorbed water on the surface of the compound. Supplementary experiment has been carried out by thermal gravity analysis, where the result is in agreement with the IR spectrum. According to the above discussion, we can draw the conclusion that there is a molecular water complex to ZnO. The molecular formula of amorphous ZnO can be simply described as $ZnO \cdot H_2O$.

Figure 5 shows a typical Raman scattering spectrum of the EPD film of amorphous ZnO. The Raman spectrum consisted of four lines. Our measurement of frequency shift of LO phonon is 584 cm^{-1}; the result is consistent with the 583 cm^{-1} previously reported.[15] The frequency lines of 331, 1147, and 1712 cm^{-1} all correspond to multiphonon processes.[15] To our knowledge, multiple phonon scattering processes were previously observed in ZnO nanocrystals.[16] For amorphous ZnO prepared by solid-state pyrolytic reaction, the resonant Raman scattering so far has not been reported in the literature. The features of the spectrum can be reasonably explained as follows: (i) amorphous ZnO are complexes with water molecules, greatly decreasing the dangling band, so the localized states were almost fully swept. (ii) The amorphous ZnO mostly displayed the characteristics of expanded states, something like that of ZnO nanocrystal, so the multiphonon resonant Raman scattering was obtained from a relatively pure amorphous ZnO with 325 nm excitation. Nevertheless, the detailed Raman analysis of the amorphous ZnO requires further study.

The PL spectrum of amorphous ZnO film is shown in Fig. 6. The amorphous ZnO shows an extremely enhanced UV emission of 300% over that of the high quality crystalline sample.[14] Two features are clearly visible from these spectra. First, the main emission peak of

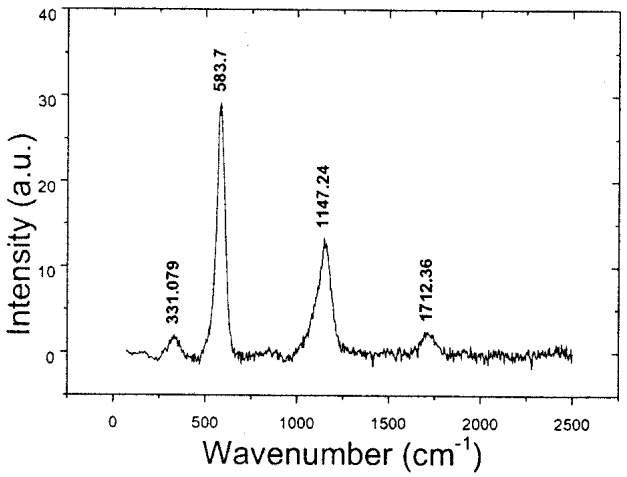

FIG. 5. Resonant Raman spectrum of typical amorphous ZnO film excited with 325 nm He-Cd laser at room temperature. The laser beam was focused on a spot of 30 μm^2.

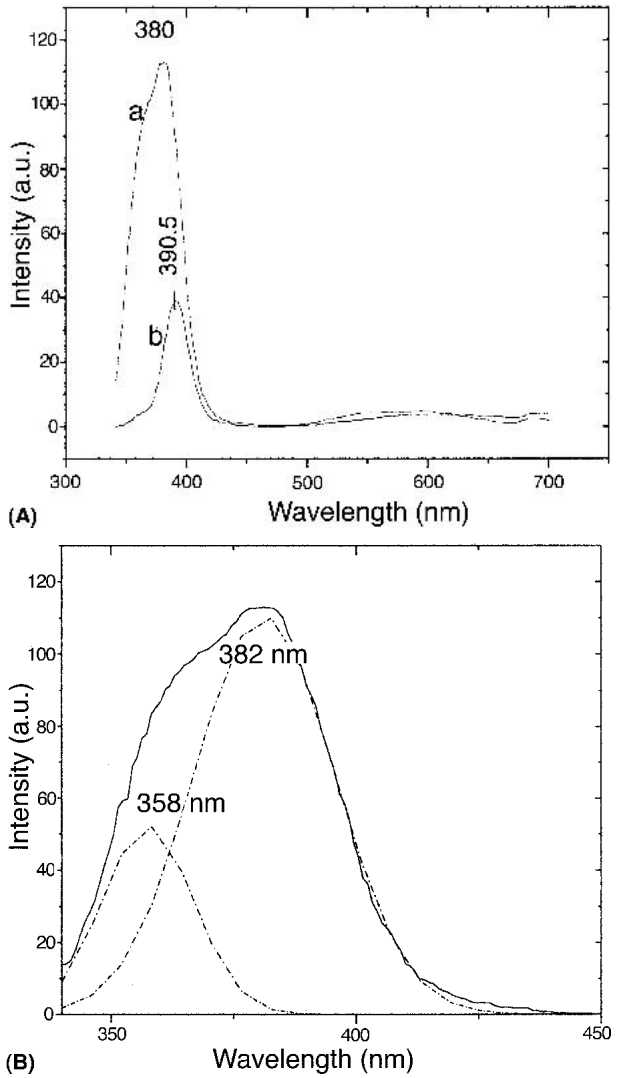

FIG. 6. (A) Room temperature steady-state PL for ZnO. (a) Amorphous ZnO (b) ZnO nanocrystallites for comparison. (B) Spectrum separation procedure of the UV emission.

amorphous ZnO is at 380 nm, a blue shift smaller than that of crystal ZnO. Second, the PL spectrum of amorphous ZnO with strong UV emission was observed while the visible emission was nearly fully quenched. The features can be explained reasonably as follows: (i) The complex H_2O sweeps the dangling band and surface defects, so only the PL spectrum with strong UV emission was observed while the visible emission was nearly fully quenched.[17] This result is in agreement with Raman spectrum. (ii) The higher degree of disorder likely leads to intensity emission stronger than that of crystalline ZnO.[14] (iii) Quantum confinement effects occur when the particle radius is of the order the exciton Bohr radius (1.8 nm, ZnO[18]). Though we did not obtain the exact diameter of amorphous ZnO from TEM and XRD, we have enough reason to believe the sizes of amorphous ZnO are smaller than 1.8 nm. Careful study of PL spectra shows that UV spectrum of amorphous ZnO consists of two kinds of emissions, while that of crystal ZnO contains only a band-edge emission. The two excitonic emissions play an important role in integrated PL intensity. The dual excitonic emissions may be derived from different emission band of amorphous ZnO. Future study of the emissive properties should lead us to a more complete description of the physical properties of the amorphous ZnO, which will help us to know more about the structure of amorphous ZnO.

IV. CONCLUSIONS

In summary, optical properties of amorphous ZnO films grown on ITO coated glass substrates by EPD were investigated. It was shown that high-quality amorphous ZnO films can dramatically increase the UV emission intensity. Raman scatting spectrum indicated that amorphous ZnO films were formed by EPD. The combination of TEM imaging and XRD spectra comparison of experimental IR spectrum and XPS experimental results provided a self-consistent description that amorphous ZnO was formed by thermal decomposition of a mixture of $Zn(CH_3COO)_2 \cdot 2H_2O$ and $NaHCO_3$. The complex water sweeps the dangling band and surface defects of amorphous ZnO; hence, the sample shows obviously quasi-three-dimensional quantum confinement effects, greatly increasing the UV emission intensity while the visible emission is barely observed at room temperature. In addition, future study of dual excitonic emission will help us to understand more about the structure of amorphous ZnO and corresponding PL properties.

ACKNOWLEDGMENTS

This work was supported by the Innovation Funds of the Chinese Academy of Sciences. We thank Zhongsu Guan and other members for their assistance in the use of XPS, TEM, XRD, and PL facilities.

REFERENCES

1. C. Klingshirn, Phys. Status. Solidi B **71,** 547 (1975).
2. H. Michael, M.H. Huang, S. Mao, H. Feick, H. Yan, Y. Wu, H. Kind, E. Weber, R. Russo, and P. Yang, Nature **292,** 1897 (2001).
3. D.C. Reynolds, D.C. Look, and B. Jogai, Solid State Commun. **99,** 873 (1996).
4. C.R. Gorla, N.W. Emanetoglu, S. Liang, W.E. Mayo, Y. Lu, M. Wraback, and H. Shen, J. Appl. Phys. **85,** 2595 (1999).
5. Y. Liu, C.R. Gorla, S. Liang, N. Emanetoglu, Y. Lu, H. Shen, and M. Wraback, J. Electron. Mater **29,** 69 (2000).
6. N.J. Dayan, S.R. Sainkar, R.N. Karekar, and R.C. Aiyer, Thin Solid Films **325,** 254 (1998).
7. C.R. Gorla, N.W. Emanetoglu, S. Liang, W.E. Mayo, Y. Liu, M. Wraback, and H. Shen, J. Appl. Phys. **85,** 2595 (1999).

8. Y. Chen, D.M. Bagnal, Z. Zhu, T. Sekiuchi, K. Park, K. Hiraga, T. Yao, S. Koyama, M.Y. Shen, and T. Goto, J. Cryst. Growth. **181,** 165 (1997).
9. B.P. Zhang, Y. Segawa, K. Wakatsuki, Y. Kashiwaba, and K. Haga, Appl. Phys. Lett. **79,** 3953 (2001).
10. T.A. Polley and W.B. Carter, Thin Solid Films **384,** 177 (2001).
11. S. Hayamizu, H. Tabata, H. Tanaka, and T. Kawai, J. Appl. Phys. **80,** 787 (1996).
12. E.M. Wong and P.C. Searson, Appl. Phys. Lett. **74,** 2939 (1999).
13. M.J. Shane, J.B. Talbot, B.G. Kinney, E. Sluzky, and K.R. Hesse, J. Colloid Interface Sci. **165,** 334 (1994).
14. H-M. Zhang and Z-J. Wang. Nanotechnology **13,** (2002).
15. T.C. Damen, S.P. Porto, and B. Tell, Phys. Rev. **142,** 570 (1966).
16. J.F. Scott, Phys. Rev. B **2,** 1209 (1970).
17. Y. Sun, J.B. Ketterson, and G.K.L. Wong, Appl. Phys. Lett. **77,** 2322 (2000).
18. A. van Dijken, J. Markkinje, and A. Meijerink, J. Lumin. **92,** 323 (2001).